electronics

MDPI

Article

A Novel Solution Methodology Based on a Modified Gradient-Based Optimizer for Parameter Estimation of Photovoltaic Models

Mohamed H. Hassan [1], Salah Kamel [1], M. A. El-Dabah [2] and Hegazy Rezk [3,4,*]

[1] Department of Electrical Engineering, Faculty of Engineering, Aswan University, Aswan 81542, Egypt; mohamedhosnymoee@gmail.com (M.H.H.); skamel@aswu.edu.eg (S.K.)
[2] Electrical Engineering Department, Faculty of Engineering, Al-AZHAR University, Cairo 11651, Egypt; Dr_mdabah@azhar.edu.eg
[3] College of Engineering at Wadi Addawaser, Prince Sattam Bin Abdulaziz University, Wadi Addawaser 11991, Saudi Arabia
[4] Electrical Engineering Department, Faculty of Engineering, Minia University, Minia 61517, Egypt
* Correspondence: hr.hussien@psau.edu.sa

Abstract: In this paper, a modified version of a recent optimization algorithm called gradient-based optimizer (GBO) is proposed with the aim of improving its performance. Both the original gradient-based optimizer and the modified version, MGBO, are utilized for estimating the parameters of Photovoltaic models. The MGBO has the advantages of accelerated convergence rate as well as avoiding the local optima. These features make it compatible for investigating its performance in one of the nonlinear optimization problems like Photovoltaic model parameters estimation. The MGBO is used for the identification of parameters of different Photovoltaic models; single-diode, double-diode, and PV module. To obtain a generic Photovoltaic model, it is required to fit the experimentally obtained data. During the optimization process, the unknown parameters of the PV model are used as a decision variable whereas the root means squared error between the measured and estimated data is used as a cost function. The results verified the fast conversion rate and precision of the MGBO over other recently reported algorithms in solving the studied optimization problem.

Keywords: modified gradient-based optimizer; parameter estimation; photovoltaic; single-diode; double-diode; PV module

Citation: Hassan, M.H.; Kamel, S.; El-Dabah, M.A.; Rezk, H. A Novel Solution Methodology Based on a Modified Gradient-Based Optimizer for Parameter Estimation of Photovoltaic Models. *Electronics* **2021**, *10*, 472. https://doi.org/10.3390/electronics10040472

Academic Editors: François Auger, Sonia Leva and Saeid Gholami Farkoush

Received: 26 December 2020
Accepted: 13 February 2021
Published: 16 February 2021

1. Introduction

Fossil fuel depletion, greenhouse gas emission, and fluctuation of fuel prices in addition to the increased demand for electrical energy are the driving forces to exploit Renewable Energy Sources (RES). One of the most promising RES technologies is solar Photovoltaic (PV). There is a wide increase of installed capacities of PV where it is expected to reach 2.8 TW by 2030 and would reach 8.59 TW in 2050 according to an international renewable energy agency (IRENA) [1].

The modeling of the PV cell/module is not quite simple as it is based on variable operating conditions like temperature and solar irradiance. Moreover, the missed parameters and the data are not provided in the manufacturers' datasheets. In addition to the urgent need for accurate modeling especially with the wide increase of PV installed capacities. The PV model expresses the nonlinear relationship between the PV cell current, voltage, and power [2]. The ideal model of a PV cell comprises a current source that represents the photo-generated current, which is a function of the solar irradiance. However, there is a deviation from this model due to variant types of loss in PV cells. One of these losses is the recombination and diffusion loss in the quasi-neutral junction. The model that considers this type of loss and the simplest equivalent circuit model is the single diode model (SDM) [3]. However, at the low irradiance level and with temperature variations,

the accuracy of obtained parameters decreased significantly [4,5]. On the other hand, the double diode model (DDM) is more accurate as it takes the loss of both the quasi-neutral and space charge junctions. According to this model, there are seven estimated parameters, which are the photo-generated current, the reverse saturation current of both diodes, and its ideality factors in addition to the shunt resistance and series resistances.

According to the literature conducted on this topic, PV modeling methods can be classified into analytical, numerical, and hybrid techniques. The former is the easiest in implementation besides it requires less computational effort. It employs the current-voltage (I-V) and power-voltage (P-V) data curves in addition to selective data from the PV cell/module datasheet for the mathematical formulation of the PV parameters estimation problem [6–9]. However, the analytical methods are based on simplifications of used mathematical formulas which will affect accuracy significantly. Moreover, this accuracy will probably be affected by the selection of the initial guess from the I-V curve. Alternatively, the Newton–Raphson [10] and Levenberg–Marquardt [11] are examples of iterative techniques are used numerical (deterministic) methods struggle from locally optimal problems in addition to the large computation time to reach the global optima as their performance governed by the initially selected solution. Conversely, the numerical (metaheuristic) evolutionary and hybrid algorithms are capable of escaping from local optima and reaching the global optimum solution easily. As per the literature, there are many metaheuristic optimization algorithms used in the estimation of PV parameters estimation, such as: Particle Swarm Optimization (PSO) [12], Artificial Bee Colony (ABC) [13], Real Coded Genetic Algorithm (RCGA) [14], Cuckoo Search (CS) [15], Biogeography-based Heterogeneous Cuckoo Search (BHCS) [16], Firefly Algorithm (FA) [17], Moth-Flame Optimization Algorithm (MFOA) [18], Bee Pollinator Flower Pollination Algorithm (BPFPA) [19], Pattern Search (PS) [20], Harmony Search (HS) [21], Fish Swarm Algorithm (FSA) [22], Ant Lion Optimizer (ALO) [23], Water Cycle Algorithm (WCA) [24], Jaya algorithm [25], Hybridized Interior Search Algorithm (HISA) [26], Artificial Immune System (AIS) [27], Salp Swarm Algorithm (SSA) [28], Artificial Biogeography based Optimization Algorithm with Mutation (BOA-M) [29], Elephant Herd Algorithm (EHA) [30], an Artificial Bee Colony-Differential Evolution (ABC-DE) [31], improved adaptive Nelder-Mead Simplex(NMS) hybridized with ABC algorithm, hybrid EHA-NMS [32], Improved Adaptive DE (IADE) [33], Chaotic Asexual Reproduction Optimization (CARO) [34], Improved Shuffled Complex Evolution (ISCE) [35], Heterogeneous Comprehensive Learning Particle Swarm Optimizer (HCLPSO) [36], Mutative-scale Parallel Chaos Optimization Algorithm (MPCOA) [37], Artificial Ecosystem optimization [38], Marine Predators Algorithm (MPA) [39], Enhanced Teaching–Learning-Based Optimization (ETLBO) algorithm [40], Coyote Optimization Algorithm (COA) [41], Harris Hawk Optimization (HHO) [42], Sunflower Optimization (SFO) [4], Grasshopper Optimization Algorithm (GOA) [43], Gravitational Search Algorithm (GSA) [44], and Improved Moths-Flames Optimization (IMFO) [45].

Although no optimization algorithm can reach the global optimum for all optimization problems as per the no-free launch theorem [46]. The GBO has the advantages of accelerated convergence rate in addition to evading from the local optima. The performance of the MGBO technique has been evaluated using the identification of parameters of different Photovoltaic models; SDM, DDM, and PV module models. The obtained results confirm the effectiveness and superiority of the MGBO to solve this problem, compared with traditional GBO and other optimization algorithms.

The main contributions of this paper can be summarized in the following points:

- Proposing a modified version of gradient-based optimizer with the aim of improving its performance and avoiding the local optima.
- Applying the original GBO and MGBO for parameter extraction of different PV models, single-diode, double-diode, and PV module.
- A comparison study on the performance of the MGBO with the original GBO and other well-known optimization techniques.

- The results prove that the MGBO has the capability to improve the performance of the original GBO with better solutions and a fast convergence rate.

This paper will be organized as follows; the mathematical formulation of PV models will be introduced in Section 2 while Section 3 will present an overview of the MGBO optimizer. In Section 4, the numerical simulation of MGBO for parameter extraction of single, double, and PV module models will take place. Finally, Section 5 outlines the main findings of this research work.

2. Mathematical Formulation

The mathematical formulation of the PV cell/module equivalent circuit parameters extraction and objected function formulation will be presented in this section.

2.1. Equivalent Circuit Model of PV Cell/Module

There are three popular equivalent circuit models of the PV cell which are SDM, DDM, and PV module model. In comparison with DDM, the PV module consumes more execution time as it is required to extract more parameters than DDM. The difference between the cost functions in the two models is relatively small [47]. In the following subsections, the equivalent circuit model of SDM, DDM, and PV module models will be shown.

2.1.1. Single Diode Model of Solar Cell

The equivalent circuit of the PV single diode model is shown in Figure 1. The output current I_L can be computed as a function of the output voltage from the following equation [48,49]:

$$I_L = I_{ph} - I_{sd} \times \left[\exp\left(\frac{V_L + I_L \times R_s}{n \times V_t} - 1\right)\right] - \frac{(V_L + I_L \times R_s)}{R_{sh}} \quad (1)$$

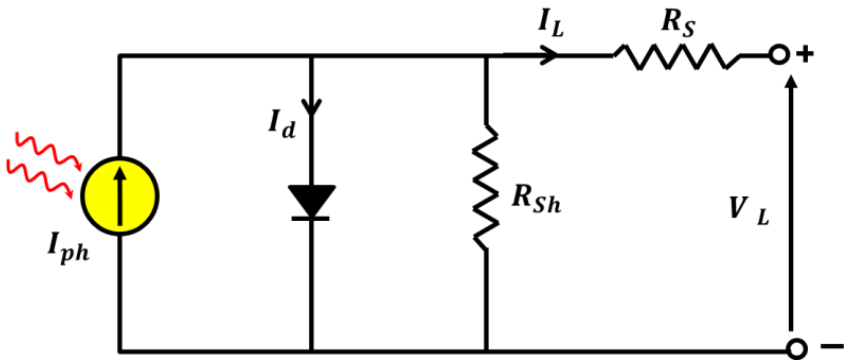

Figure 1. Schematics of single diode model.

2.1.2. Double Diode Model of Solar Cell

The accuracy of the PV model can be enhanced by adding another diode that reflects the space charge loss in addition to diffusion and recombination loss considered in SDM. The DDM equivalent circuit PV model is depicted in Figure 2. The following equation can be used for output current calculation:

$$I_L = I_{ph} - I_{sd,1} \times \left[\exp\left(\frac{V_L + I_L \times R_s}{n_1 \times V_t} - 1\right)\right] - I_{sd,2} \times \left[\exp\left(\frac{V_L + I_L \times R_s}{n_2 \times V_t} - 1\right)\right] - \frac{(V_L + I_L \times R_s)}{R_{sh}} \quad (2)$$

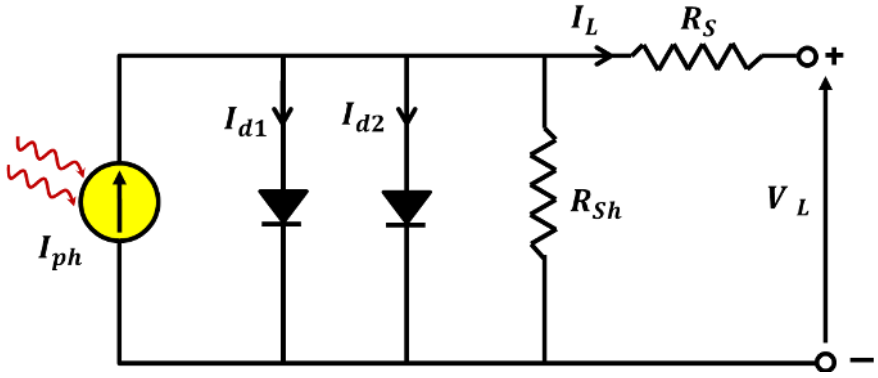

Figure 2. Schematics of the double diode model.

2.1.3. PV Module Model

Calculation of the output current of the PV module model in Figure 3 can be attained using the following equation:

$$I_L/N_P = I_{ph} - I_{sd} \times \left[\exp\left(\frac{(V_L/N_S + I_L \times R_s/N_P)}{n \times V_t} - 1\right)\right] - \frac{(V_L/N_S + I_L \times R_s/N_P)}{R_{sh}} \quad (3)$$

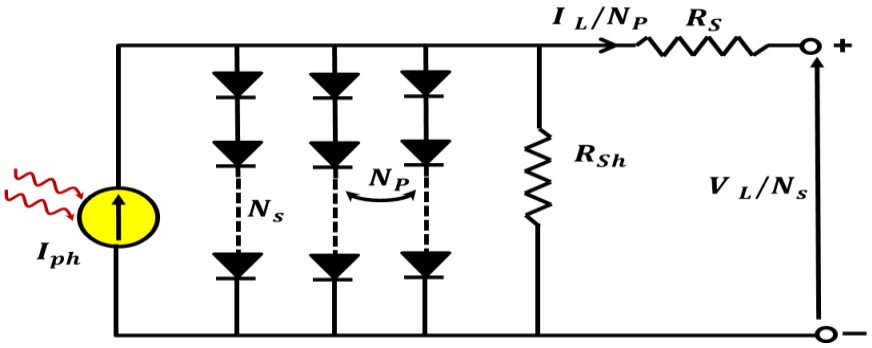

Figure 3. Equivalent circuit model of the PV module model.

2.2. Objective Function Formulation

For a precise estimation of the different used PV model, the objective function is essentially defined. It will be used for the evaluation of the optimizer performance, in addition to guaranteeing the estimated parameter accuracy. In this research, the root means square error (RMSE) between the experimental and estimated current will be used as a cost function as given in Equation (4) [50].

$$RMSE(x) = \sqrt{\frac{1}{N}\sum_{m=1}^{N}[f(V_m, I_m, x) - I_m]^2} \quad (4)$$

where x is the vector of estimated parameters that are $\{I_{ph},\ I_{sd,1},\ I_{sd,2},\ R_S,\ R_{sh},\ n_1,\ n_2\}$ in case of DDM and $x = \{I_{ph},\ I_{sd},\ R_S,\ R_{sh},\ n\}$ in the case of SDM, and N is the number of measured values. The $f(V_m,\ I_m,\ x)$ are used for the current calculation from Equations (1)–(3).

3. Overview of GBO

The gradient-based optimizer (GBO) is a proposed metaheuristic optimization algorithm by (Iman Ahmadianfar et al., 2020) [51]. It was inspired by Newton's gradient-based method. This optimization algorithm has a unique feature as it results from the combination of gradient-based methods and population methods concepts. This feature makes

the GBO an efficient and effective optimization algorithm as it will be capable of escaping from the local optimum problem besides the fast convergence rate. To explore the search space, the GBO uses two operators namely Gradient Search Rule (GSR) and Local Escaping Operator (LEO) in addition to a set of vectors.

3.1. GBO Initialization

The GBO comprises an N vector (members of populations) in the D-dimensional search space as Equation (5) where members of the population are randomly generated by Equation (6).

$$X_{n,d} = [X_{n,1},\ X_{n,1}, \ldots, X_{n,D}] \quad n = 1, 2, \ldots, N \quad d = 1, 2, \ldots, D \tag{5}$$

$$X_n = X_{min} + rand(0,1) \times (X_{max} - X_{min}) \tag{6}$$

where X_{min}, X_{max} the border are limits of the decision variables and $rand(0,\ 1)$ is a randomly generated number in the range of (0, 1).

3.2. Gradient Search Rule (GSR)

GSR is based on the concept of the gradient-based method where the extreme point at which the gradient is equal to zero must be identified to determine the optimal solution. Exploration tendency enhancement and convergence rate acceleration are the aims of using GSR. Based on the numerical gradient approach and with the aids of the Taylor series, the new position X_{n+1} can be obtained by:

$$X_{n+1} = X_n - \frac{2\Delta x \times f(X_n)}{f(X_n + \Delta x) - f(X_n - \Delta x)} \tag{7}$$

Equation (7) will be changed to accommodate the population-based search concept which is given by Equation (8).

$$GSR = randn \times \frac{2\Delta x \times X_n}{(x_{worst} - x_{best} + \varepsilon)} \tag{8}$$

where x_{worst}, x_{best} are the worst and best candidate solutions through the process of optimization, $randn$ is a normally distributed random number, ε is a small number arbitrarily choose in the range of [0, 0.1], and Δx is the change in position at each iteration.

To achieve the balance between the exploration and exploitation process and seeking for search capability improvement, the GSR will be modified accordingly to be:

$$GSR = randn \times \rho_1 \times \frac{2\Delta x \times X_n}{(x_{worst} - x_{best} + \varepsilon)} \tag{9}$$

where the randomly generated parameter ρ_1 is given by:

$$\rho_1 = (2 \times rand \times \alpha) - \alpha \tag{10}$$

$$\alpha = \left| \beta \times \sin\left(\frac{3\pi}{2} + \sin\left(\beta \times \frac{3\pi}{2} \right) \right) \right| \tag{11}$$

$$\beta = \beta_{min} + (\beta_{min} - \beta_{min}) \times \left(1 - \left(\frac{m}{M} \right)^3 \right)^2 \tag{12}$$

where β_{min} and β_{max} are 0.2 and 1.2, respectively, m is the number of iterations, and M is the total number of iterations. The symbol α is a sine function for the transition from exploration to exploitation. In addition, $randn$ is a normally distributed random number,

and ε is a small number within the range of [0, 0.1]. The change Δx between the best candidate solution x_{best} and a randomly selected position x_{r1}^m is given by:

$$\Delta x = rand(1:N) \times |step| \tag{13}$$

$$step = \frac{(x_{best} - x_{r1}^m) + \delta}{2} \tag{14}$$

$$\delta = 2 \times rand \times \left(\left| \frac{x_{r1}^m + x_{r2}^m + x_{r3}^m + x_{r4}^m}{4} \right| - x_n^m \right) \tag{15}$$

where $rand(1:N)$ is a random number with N dimensions, $r1$, $r2$, $r3$, and $r4$ ($r1 \neq r2 \neq r3 \neq r4 \neq n$) are different integers randomly chosen from [1, N], $step$ is a step size, which is determined by x_{best} and x_{r1}^m.The updated position X_{n+1} in Equation (7) can be updated based on the GSR as given in Equation (16):

$$X_{n+1} = X_n - GSR \tag{16}$$

For better exploitation of the nearby area of X_n, the direction of movement (DM) is added, which is calculated as below:

$$DM = rand \times \rho_2 \times (x_{best} - x_n) \tag{17}$$

$$\rho_2 = (2 \times rand \times \alpha) - \alpha \tag{18}$$

Equation (19) is used to obtain the updated position taking into consideration the GSR and DM.

$$X1_n^m = x_n^m - \mathrm{GSR} + \mathrm{DM} \tag{19}$$

$$X1_n^m = x_n^m - \mathrm{GSR} + \mathrm{DM} \tag{20}$$

$$X1_n^m = x_n^m - randn \times \rho_1 \times \frac{2\Delta x \times x_n^m}{(x_{worst} - x_{best} + \varepsilon)} + rand \times \rho_2 \times (x_{best} - x_n^m) \tag{21}$$

By replacing the position of the best vector (x_{best}) with the current vector (x_n^m) in Equation (21), the new vector ($X2_n^m$) can be generated as follows:

$$X2_n^m = x_{best} - randn \times \rho_1 \times \frac{2\Delta x \times x_n^m}{(yp_n^m - yq_n^m + \varepsilon)} + rand \times \rho_2 \times (x_{r1}^m - x_{r2}^m) \tag{22}$$

in which

$$yp_n = rand \times \left(\frac{[z_{n+1} + x_n]}{2} + rand \times \Delta x \right) \tag{23}$$

$$yq_n = rand \times \left(\frac{[z_{n+1} + x_n]}{2} - rand \times \Delta x \right) \tag{24}$$

Based on the positions $X1_n^m$,$X2_n^m$, and the current position (X_n^m), the new solution at the next iteration (x_n^{m+1}) can be defined as

$$x_n^{m+1} = r_a \times (r_b \times X1_n^m + (1 - r_b) \times X2_n^m) + (1 - r_a) \times X3_n^m \tag{25}$$

$$X3_n^m = X_n^m - \rho_1 \times (X2_n^m - X1_n^m) \tag{26}$$

3.3. Local Escaping Operator (LEO)

The LEO is introduced to promote the efficiency of the GBO algorithm for solving complex problems. The LEO generates a solution with a superior performance (X_{LEO}^m) by using several solutions, which include the best position (x_{best}), the solutions $X1_n^m$ and $X2_n^m$, two random solutions x_{r1}^m and x_{r2}^m, and a new randomly generated solution (x_k^m). The solution X_{LEO}^m is generated by the following scheme:

$if\ rand < pr$
$\quad if\ rand < 0.5$
$X_{LEO}^m = X_n^{m+1} + f_1 \times (u_1 \times x_{best} - u_2 \times x_k^m) + f_2 \times \rho_1 \times (u_3 \times (X2_n^m - X1_n^m) + u_2 \times (x_{r1}^m - x_{r2}^m))/2$
$X_n^{m+1} = X_{LEO}^m$
$\quad$ Else

$X_{LEO}^m = x_{best} + f_1 \times (u_1 \times x_{best} - u_2 \times x_k^m) + f_2 \times \rho_1 \times (u_3 \times (X2_n^m - X1_n^m) + u_2 \times (x_{r1}^m - x_{r2}^m))/2$
$X_n^{m+1} = X_{LEO}^m$
$\quad$ End
End

where f_1 is a uniform random number in the range of $(-1, 1)$, f_2 is a random number from a normal distribution with a mean of 0 and a standard deviation of 1, pr is the probability, and u_1, u_2, and u_3 are three random numbers, which are defined as:

$$u_1 = \begin{cases} 2 \times rand & if\ \mu_1 < 0.5 \\ 1 & otherwise \end{cases} \tag{27}$$

$$u_2 = \begin{cases} rand & if\ \mu_1 < 0.5 \\ 1 & otherwise \end{cases} \tag{28}$$

$$u_3 = \begin{cases} rand & if\ \mu_1 < 0.5 \\ 1 & otherwise \end{cases} \tag{29}$$

where $rand$ is a random number in the range of (0, 1), and μ_1 is a number in the range of (0, 1). The above equations can be simplified:

$$u_1 = L_1 \times 2 \times rand + (1 - L_1) \tag{30}$$

$$u_2 = L_1 \times rand + (1 - L_1) \tag{31}$$

$$u_3 = L_1 \times rand + (1 - L_1) \tag{32}$$

where L_1 is a binary parameter with a value of 0 or 1. If parameter μ_1 is less than 0.5, the value of L_1 is 1, otherwise, it is 0. To determine the solution x_k^m in Equation (6), the following scheme is suggested.

$$x_k^m = \begin{cases} x_{rand} & if\ \mu_2 < 0.5 \\ x_p^m & otherwise \end{cases} \tag{33}$$

$$x_{rand} = X_{min} + rand(0,\ 1) \times (X_{max} - X_{min}) \tag{34}$$

where x_{rand} is a new solution, x_p^m is a randomly selected solution of the population ($p \in [1, 2, \ldots, N]$), and μ_2 is a random number in the range of (0, 1). Equations (6)–(7) can be simplified as:

$$x_k^m = L_2 \times x_p^m + (1 - L_2) \times x_{rand} \tag{35}$$

where L_2 is a binary parameter with a value of 0 or 1. If μ_2 is less than 0.5, the value of L_2 is 1, otherwise, it is 0.

3.4. Modified GBO

One of the methods for enhancing the performance of optimization algorithms seeking to obtain the best solution and decreasing the search space is to find the stability between the capability of exploitation and exploration [52]. The convergence of a technique depends on how the solutions are moved in the search space. In the GBO algorithm, the direction of movement (DM) is used to converge around the area of the solution. Therefore, we suggest changing the DM-value gradually in the MGBO according to:

$$DM = rand \times D \times \rho_2 \times (x_{best} - x_n) \tag{36}$$

where D value increases gradually from 1 to 2 as follows [53]:

$$D_i = 2 - (1 - \frac{i}{N})^2 \quad (37)$$

The same modification has been used to improve the balancing between exploration and exploitation phases in the search process of water cycle algorithm in [53]. The flow chart of the MGBO algorithm is summarized in Figure 4.

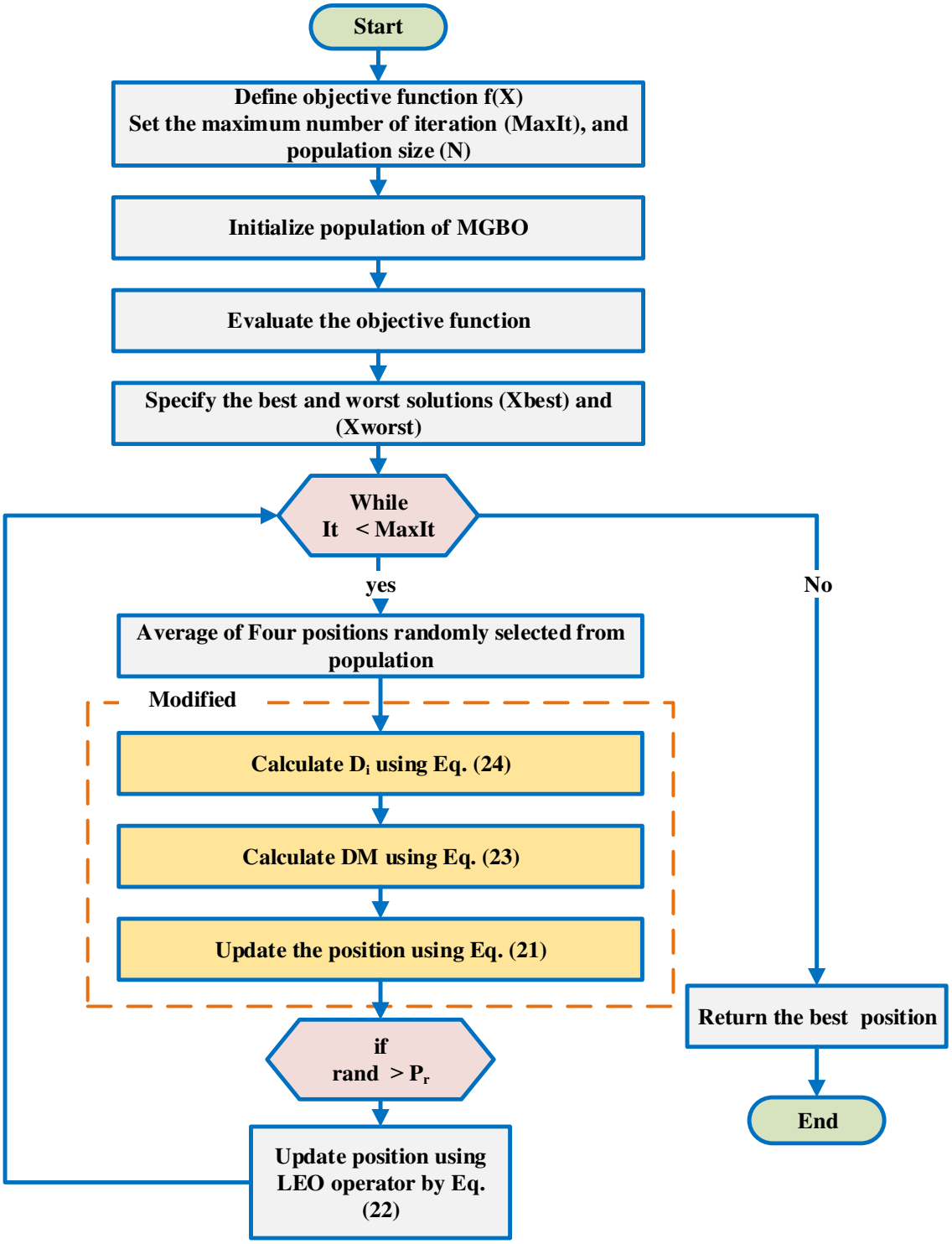

Figure 4. The flow chart of the modified gradient-based optimizer (MGBO) algorithm.

4. Results and Evaluation

The numerical simulation of the MGBO for estimating parameters of single-diode, double-diode, and PV-Module models is illustrated in this section. As mentioned previously, the root means squared value of the error (RMSE) between measures and correspondingly estimated current is used as a cost function in this research. The MGBO-based parameters estimation is accomplished using MATLAB 2016a platform using an Intel® core TM i5-4210U CPU, 1.70 GHz, 8 GB RAM Laptop. Table 1 lists the boundary limits of the estimated parameters of all used PV models in this research.

Table 1. Parameters boundary of different PV models.

Parameter	Single Diode/Double Diode		PV Module	
	Lower Bound	Upper Bound	Lower Bound	Upper Bound
I_{ph} (A)	0	1	0	2
I_{sd}, I_{sd1}, I_{sd2} (μA)	0	1	0	5
R_S (Ω)	0	0.5	0	2
R_{sh} (Ω)	0	100	0	2000
n, n_1, n_2	1	2	1	50

4.1. Scenario #1: Single Diode Model

Parameters identification of the single diode model of PV cells will be investigated in this subsection. In comparison with recently proposed metaheuristic optimizers, the MGBO attains the lowest RMSE with a comparatively fast convergence rate as can be depicted in Figures 5 and 6. The statistical results reflect this superiority as indicated in Table 2 below. The best-attained results of the PV cell single diode model after 20 runs using MGBO and some of the different used optimization algorithms are given in Table 3. In addition, Table 4 lists the individual absolute error between measured and simulated data of the PV cell output current, output voltage, and output power. A graphical plot of the Integral absolute error (IAE) of the simulated current and output power of the PV cell single diode model using MGBO is displayed in Figure 7. The coincidence between the measured and estimated data points for the I-V and P-V curves is depicted in Figure 8a,b.

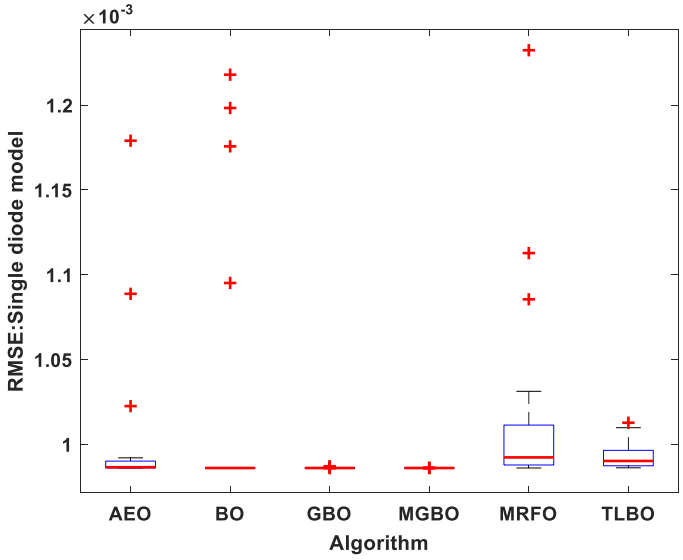

Figure 5. Best root means square error (RMSE) boxplot in 20 runs of different algorithms for the single diode model.

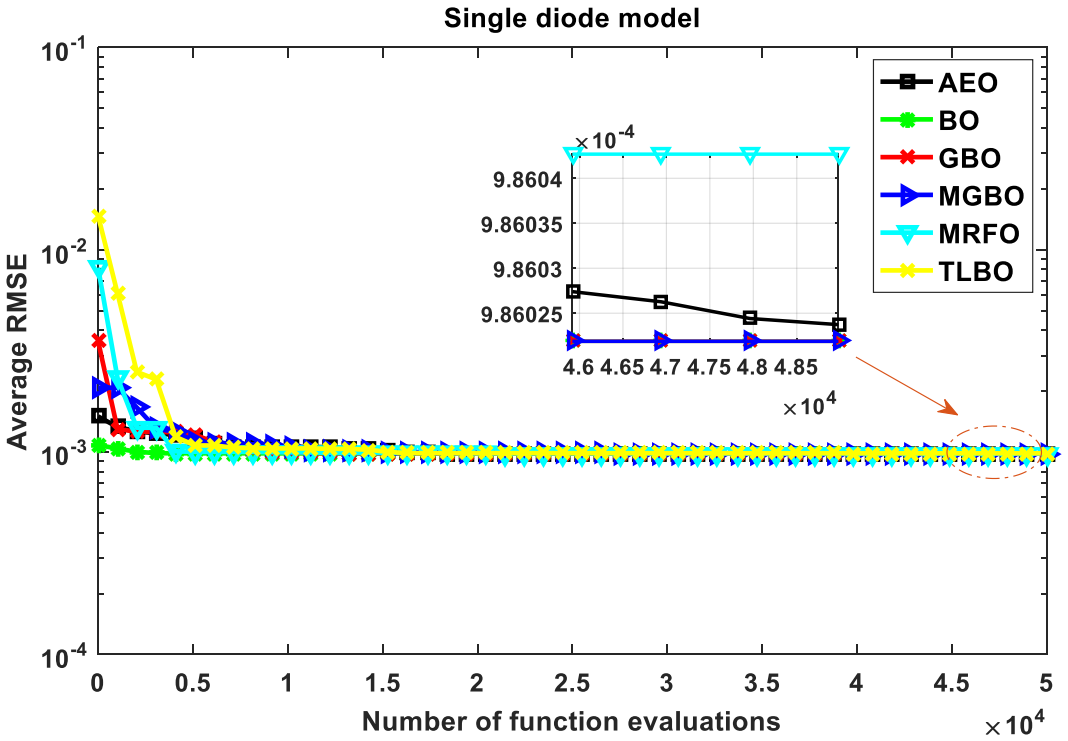

Figure 6. Convergence graphs of different algorithms for the single diode model.

Table 2. Comparisons of the statistical results of different algorithms for the single diode model.

Algorithm	RMSE				
	Min	Mean	Median	Max	SD
MGBO	9.8602×10^{-4}	9.8603×10^{-4}	9.86×10^{-4}	9.86×10^{-4}	2.25×10^{-8}
GBO	9.8602×10^{-4}	9.8611×10^{-4}	9.86×10^{-4}	9.870×10^{-4}	2.74×10^{-7}
BO	9.8602×10^{-4}	1.0232×10^{-3}	9.86×10^{-4}	1.218×10^{-3}	7.92×10^{-5}
MRFO	9.8604×10^{-4}	1.0177×10^{-3}	9.92×10^{-4}	1.232×10^{-3}	6.10×10^{-5}
TLBO	9.8616×10^{-4}	9.9315×10^{-4}	9.90×10^{-4}	1.013×10^{-3}	8.16×10^{-6}
AEO	9.8602×10^{-4}	1.0036×10^{-3}	9.86×10^{-4}	1.179×10^{-3}	4.76×10^{-5}

Table 3. Best solar cell estimated parameters for the single diode model.

Algorithm	I_{ph} (A)	I_{sd} (μA)	R_s (Ω)	R_{sh} (Ω)	n	RMSE
MGBO	0.760776	0.323021	0.036377	53.71852	1.481184	9.8602×10^{-4}
GBO	0.760776	0.323021	0.036377	53.71853	1.481184	9.8602×10^{-4}
BO	0.760776	0.323021	0.036377	53.71853	1.481184	9.8602×10^{-4}
MRFO	0.760778	0.323956	0.036365	53.76327	1.481476	9.8604×10^{-4}
TLBO	0.760773	0.324008	0.036373	53.99459	1.481486	9.8616×10^{-4}
AEO	0.760775	0.323339	0.036373	53.74679	1.481283	9.8602×10^{-4}

Table 4. Integral absolute error (IAE) of MGBO on the Single diode model.

Item	Measured Data			Simulated Current Data		Simulated Power Data	
	V (V)	I (A)	P (w)	I_{sim} (A)	IAE_I (A)	P_{sim} (W)	IAE_P (W)
1	−0.2057	0.7640	−0.157155	0.7640877	0.000087704	−0.1571728	0.000018041
2	−0.1291	0.7620	−0.098374	0.7626631	0.000663086	−0.0984598	0.000085604
3	−0.0588	0.7605	−0.044717	0.7613553	0.000855307	−0.0447677	0.000050292
4	0.0057	0.7605	0.004335	0.760154	0.000346009	0.00433288	0.000001972
5	0.0646	0.7600	0.049096	0.7590552	0.000944791	0.04903497	0.000061034

Table 4. *Cont.*

Item	Measured Data			Simulated Current Data		Simulated Power Data	
	V (V)	I (A)	P (w)	I_{sim} (A)	IAE_I (A)	P_{sim} (W)	IAE_P (W)
6	0.1185	0.7590	0.089942	0.7580423	0.000957655	0.08982802	0.000113482
7	0.1678	0.7570	0.127025	0.7570917	0.0000916534	0.12703998	0.000015379
8	0.2132	0.7570	0.161392	0.7561414	0.000858636	0.16120934	0.000183061
9	0.2545	0.7555	0.192275	0.7550869	0.000413128	0.19216961	0.000105141
10	0.2924	0.7540	0.22047	0.7536639	0.000336123	0.22037132	0.000098282
11	0.3269	0.7505	0.245338	0.751391	0.000890966	0.24562971	0.000291257
12	0.3585	0.7465	0.26762	0.7473539	0.000853851	0.26792636	0.000306105
13	0.3873	0.7385	0.286021	0.7401172	0.001617221	0.2866474	0.000626350
14	0.4137	0.7280	0.301174	0.7273822	0.000617776	0.30091803	0.000255574
15	0.4373	0.7065	0.308952	0.7069727	0.000472651	0.30915914	0.000206690
16	0.4590	0.6755	0.310055	0.6752802	0.000219849	0.30995359	0.000100911
17	0.4784	0.6320	0.302349	0.6307583	0.001241728	0.30175476	0.000594043
18	0.4960	0.5730	0.284208	0.5719284	0.001071642	0.28367647	0.000531534
19	0.5119	0.4990	0.255438	0.499607	0.000607019	0.25574883	0.000310733
20	0.5265	0.4130	0.217445	0.4136488	0.000648792	0.21778609	0.000341589
21	0.5398	0.3165	0.170847	0.3175101	0.00101011	0.17139196	0.000545257
22	0.5521	0.2120	0.117045	0.2121549	0.000154939	0.11713074	0.000085542
23	0.5633	0.1035	0.058302	0.1022513	0.001248688	0.05759816	0.000703386
24	0.5736	−0.0100	−0.005736	−0.008718	0.001282458	−0.0050004	0.000735618
25	0.5833	−0.1230	−0.071746	−0.125507	0.002507413	−0.0732085	0.001462574
26	0.5900	−0.2100	−0.1239	−0.208472	0.001527673	−0.1229987	0.000901327
Sum of IAE					0.021526869		0.008730779

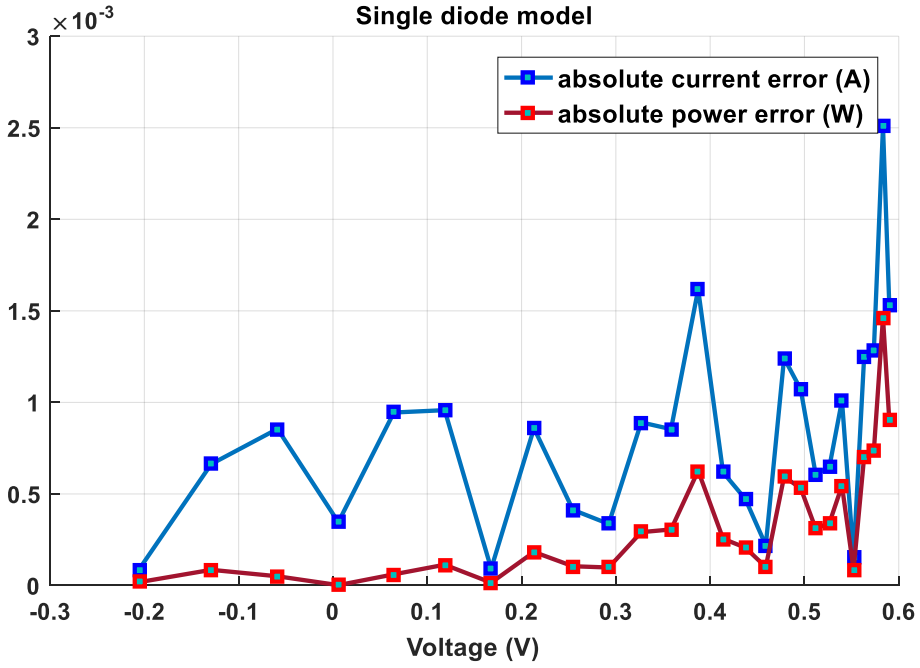

Figure 7. Individual absolute errors for current and power using MGBO (single diode model).

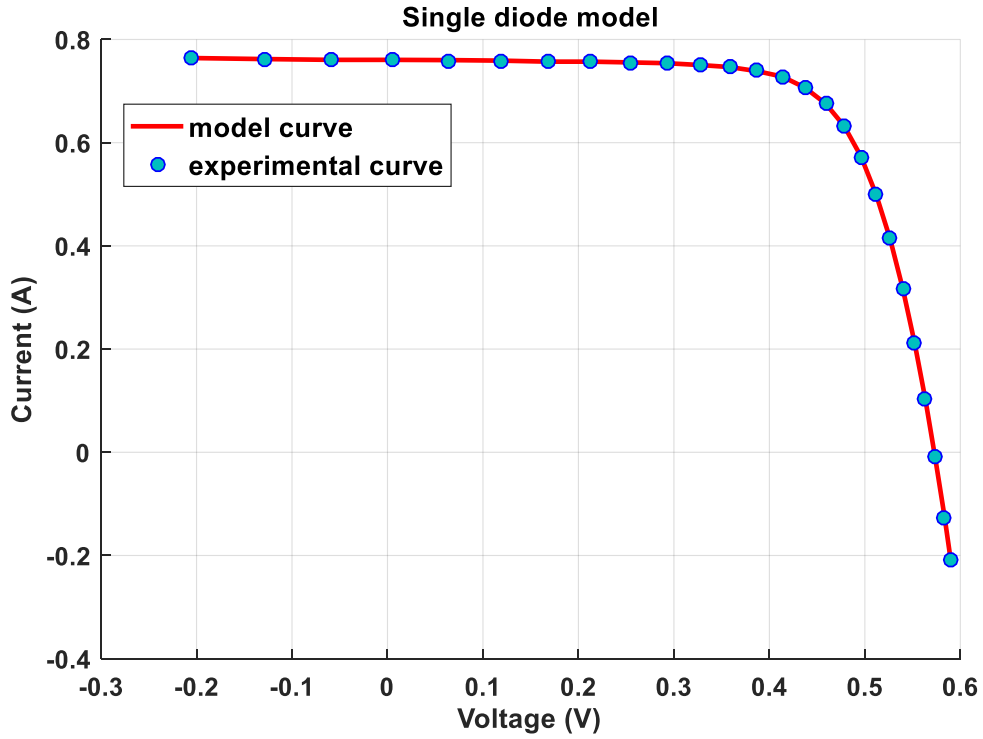

(**a**)

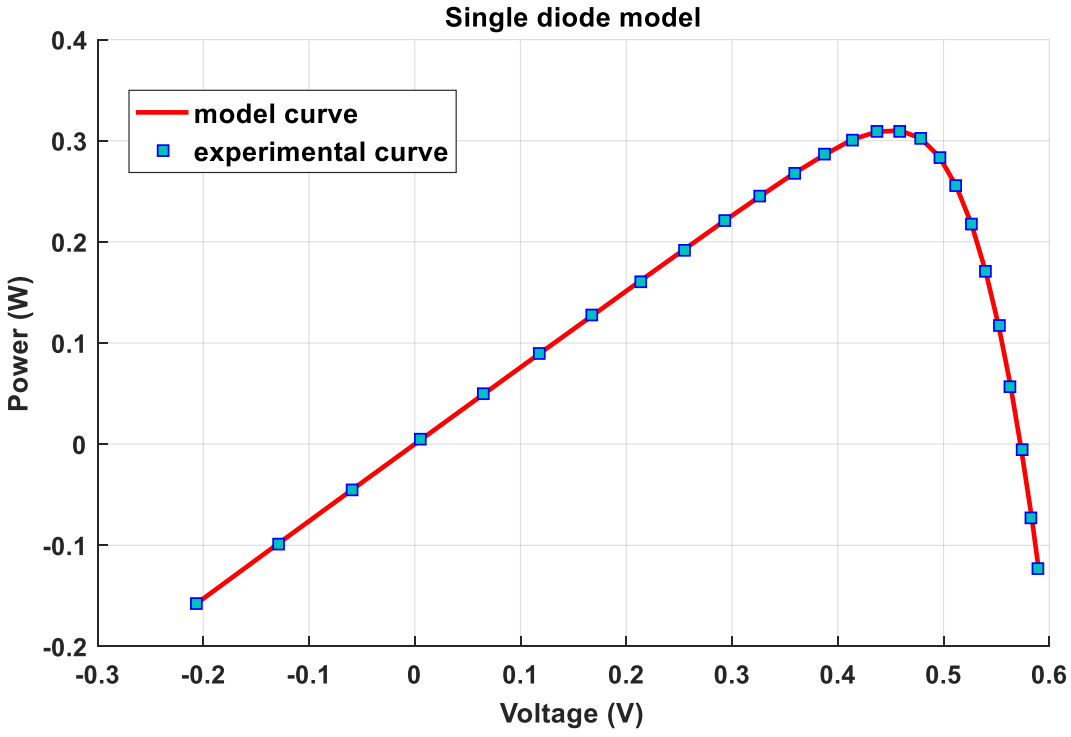

(**b**)

Figure 8. Comparisons between experimental data and simulated data obtained by MGBO for single diode model (**a**) I-V characteristics; (**b**) P-V characteristics.

4.2. Scenario #2: Double Diode Model

As mentioned previously, the DDM is more accurate than the SDM for parameters estimation of the PV cell. This subsection will be used to present this feature of the DDM in addition to the application of the MGBO and other comparative algorithms for parameters estimation of the PV cell model. The best-obtained parameters of the double diode model equivalent circuit model using MGBO and the other comparative optimization algorithms are presented in Table 5. The MGBO reaches the lowest RMSE in comparison with the other used optimizers as can be visualized in Figure 9. Furthermore, the statistical results in Table 6 stress these superiorities over the comparative algorithms besides the provided boxplot in Figure 10. Additionally, in Figure 11, the IAE of the measured and simulated current and power using the DDM of PV is tabulated in Table 7. The accurate estimation of the PV DDM parameters can be expressed by the accurate matching of the experimental and estimated I-V and P-V curves as shown in Figure 12.

Table 5. Best solar cell estimated parameters for the Double diode model.

Algorithm	I_{ph} (A)	I_{sd1} (μA)	R_s (Ω)	R_{sh} (Ω)	n_1	I_{sd2} (μA)	n_2	RMSE
MGBO	0.760778	0.226221	0.036733	55.53231	1.451161	0.739538	1.996218	9.8253×10^{-4}
GBO	0.760783	0.20525	0.036839	55.99065	1.443028	0.933745	2.000000	9.8274×10^{-4}
BO	0.760784	0.593546	0.036662	55.03379	2.000000	0.244292	1.457524	9.8266×10^{-4}
MRFO	0.760837	0.097161	0.036414	53.2903	1.697971	0.27743	1.470683	9.8677×10^{-4}
TLBO	0.760755	0.569821	0.036664	55.27114	1.962822	0.237306	1.455441	9.8314×10^{-4}
AEO	0.760773	0.306351	0.036413	54.1903	1.476753	0.131635	2.000000	9.8502×10^{-4}

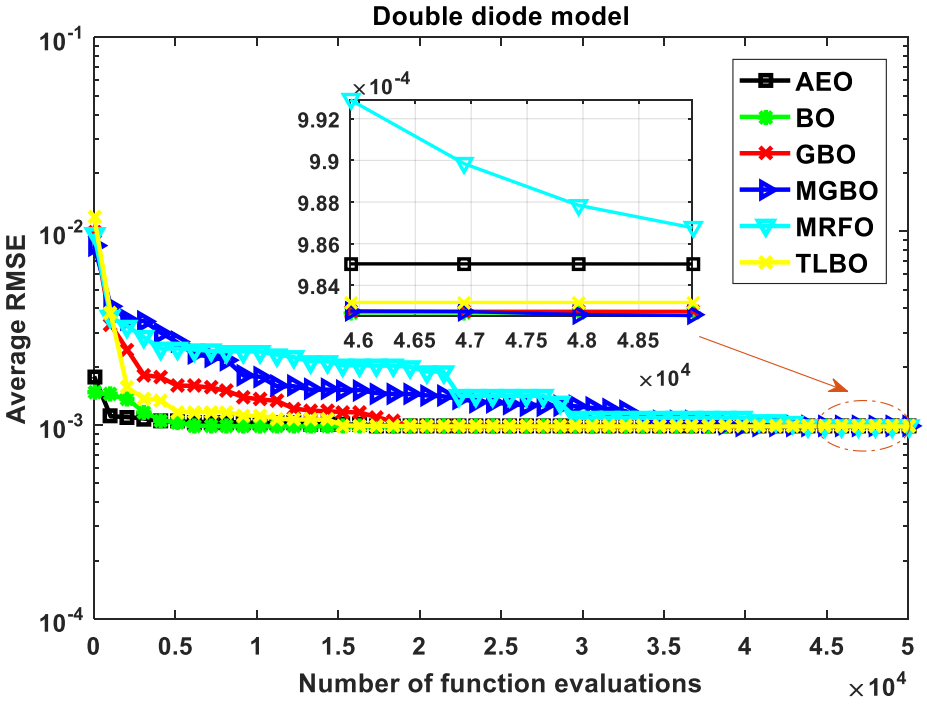

Figure 9. Convergence graphs of different algorithms for the Double diode model.

Table 6. Comparisons of the statistical results of different algorithms for the Double diode model.

Algorithm	RMSE				
	Min	**Mean**	**Median**	**Max**	**SD**
MGBO	9.8253×10^{-4}	9.8444×10^{-4}	9.8440×10^{-4}	9.8602×10^{-4}	1.29×10^{-6}
GBO	9.8274×10^{-4}	1.0160×10^{-3}	9.8640×10^{-4}	1.3800×10^{-3}	8.91×10^{-5}
BO	9.8266×10^{-4}	1.0546×10^{-3}	9.8601×10^{-4}	2.3223×10^{-3}	2.99×10^{-4}
MRFO	9.8677×10^{-4}	1.1852×10^{-3}	1.1249×10^{-3}	1.4701×10^{-3}	1.64×10^{-4}
TLBO	9.8314×10^{-4}	1.0037×10^{-3}	9.9925×10^{-4}	1.0820×10^{-3}	2.15×10^{-5}
AEO	9.8502×10^{-4}	1.0021×10^{-3}	9.9572×10^{-4}	1.0696×10^{-3}	2.12×10^{-5}

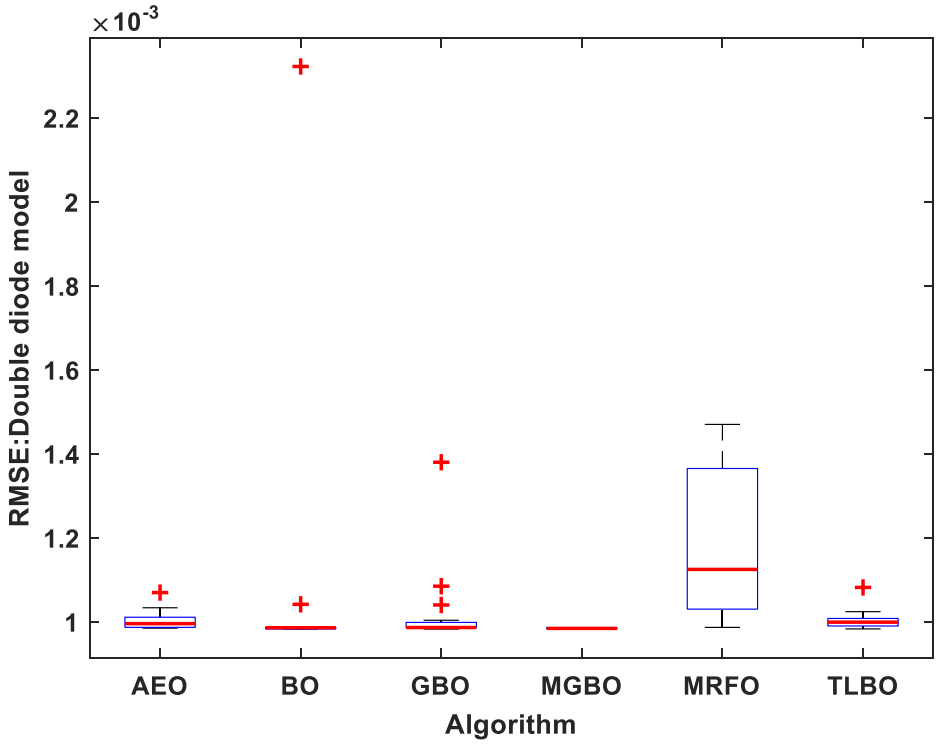

Figure 10. Best RMSE boxplot in 20 runs of different algorithms for the Double diode model.

Table 7. IAE of MGBO on the Double diode model.

Item	Measured Data			Simulated Current Data		Simulated Power Data	
	V (V)	**I (A)**	**P (w)**	$\mathbf{I_{sim}}$ **(A)**	$\mathbf{IAE_I}$ **(A)**	$\mathbf{P_{sim}}$ **(W)**	$\mathbf{IAE_P}$ **(W)**
1	−0.2057	0.7640	−0.157155	0.763977787	0.000022213	−0.1571502	0.000004569
2	−0.1291	0.7620	−0.098374	0.762599636	0.000599636	−0.0984516	0.000077413
3	−0.0588	0.7605	−0.044717	0.761334311	0.000834311	−0.0447664	0.000049057
4	0.0057	0.7605	0.004335	0.760171392	0.000328608	0.00433298	0.000001873
5	0.0646	0.7600	0.049096	0.759106204	0.000893796	0.04903826	0.000057739
6	0.1185	0.7590	0.089942	0.758120812	0.000879188	0.08983732	0.000104184
7	0.1678	0.7570	0.127025	0.757188839	0.000188839	0.12705629	0.000031687
8	0.2132	0.7570	0.161392	0.756244644	0.000755356	0.16123136	0.000161042
9	0.2545	0.7555	0.192275	0.755179094	0.000320906	0.19219308	0.000081671

Table 7. *Cont.*

Item	Measured Data			Simulated Current Data		Simulated Power Data	
	V (V)	I (A)	P (w)	I_{sim} (A)	IAE_I (A)	P_{sim} (W)	IAE_P (W)
10	0.2924	0.7540	0.22047	0.753724777	0.000275223	0.22038912	0.000080475
11	0.3269	0.7505	0.245338	0.751401912	0.000901912	0.24563329	0.000294835
12	0.3585	0.7465	0.26762	0.747304101	0.000804101	0.26790852	0.000288270
13	0.3873	0.7385	0.286021	0.740012525	0.001512525	0.28660685	0.000585801
14	0.4137	0.7280	0.301174	0.727247276	0.000752724	0.3008622	0.000311402
15	0.4373	0.7065	0.308952	0.706848564	0.000348564	0.30910488	0.000152427
16	0.4590	0.6755	0.310055	0.675206706	0.000293294	0.30991988	0.000134622
17	0.4784	0.6320	0.302349	0.630755525	0.001244475	0.30175344	0.000595357
18	0.4960	0.5730	0.284208	0.571989313	0.001010687	0.2837067	0.000501301
19	0.5119	0.4990	0.255438	0.499701818	0.000701818	0.25579736	0.000359261
20	0.5265	0.4130	0.217445	0.413731565	0.000731565	0.21782967	0.000385169
21	0.5398	0.3165	0.170847	0.317546550	0.001046550	0.17141163	0.000564928
22	0.5521	0.2120	0.117045	0.212125269	0.000125269	0.11711436	0.000069161
23	0.5633	0.1035	0.058302	0.102165984	0.001334016	0.0575501	0.000751451
24	0.5736	−0.0100	−0.005736	−0.00879142	0.001208580	−0.0050427	0.000693241
25	0.5833	−0.1230	−0.071746	−0.12554747	0.002547470	−0.0732318	0.001485939
26	0.5900	−0.2100	−0.1239	−0.20838191	0.001618088	−0.1229453	0.000954672
Sum of IAE					0.021279712		0.008777547

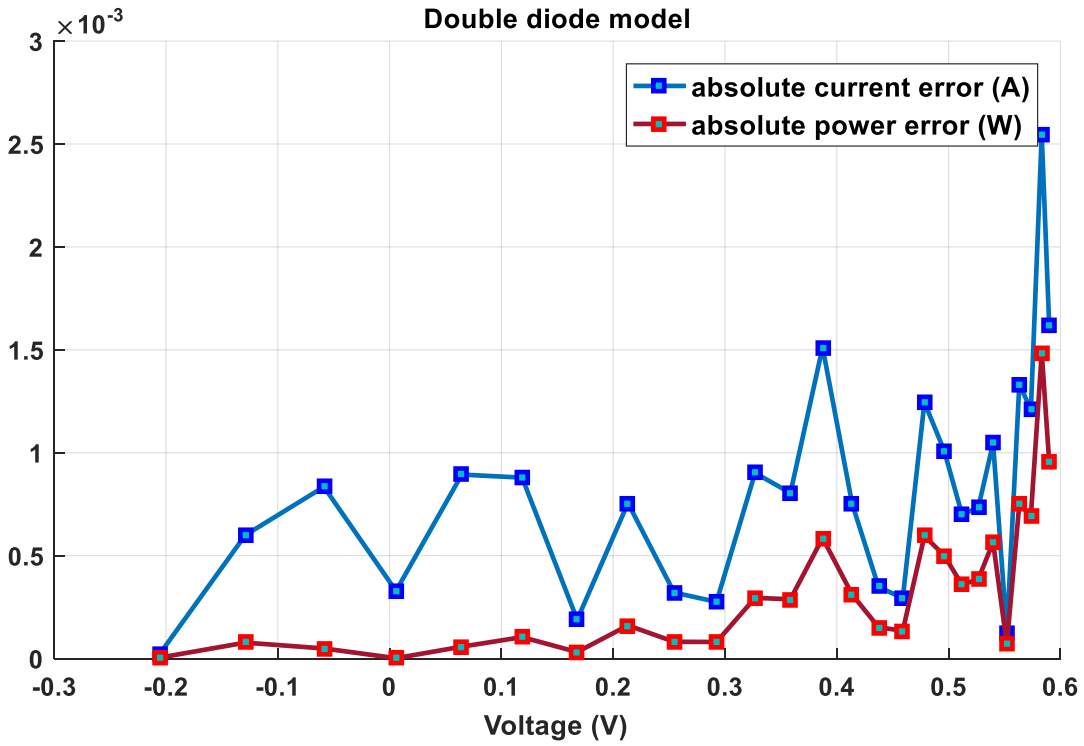

Figure 11. Individual absolute errors for current and power using MGBO (Double diode model).

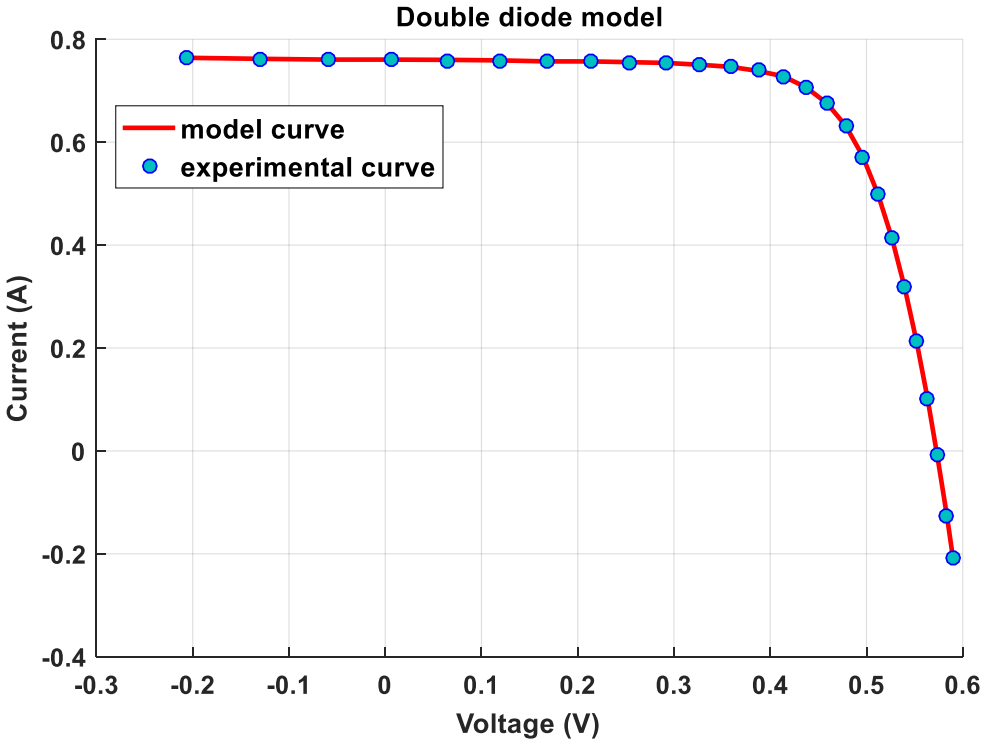

(**a**)

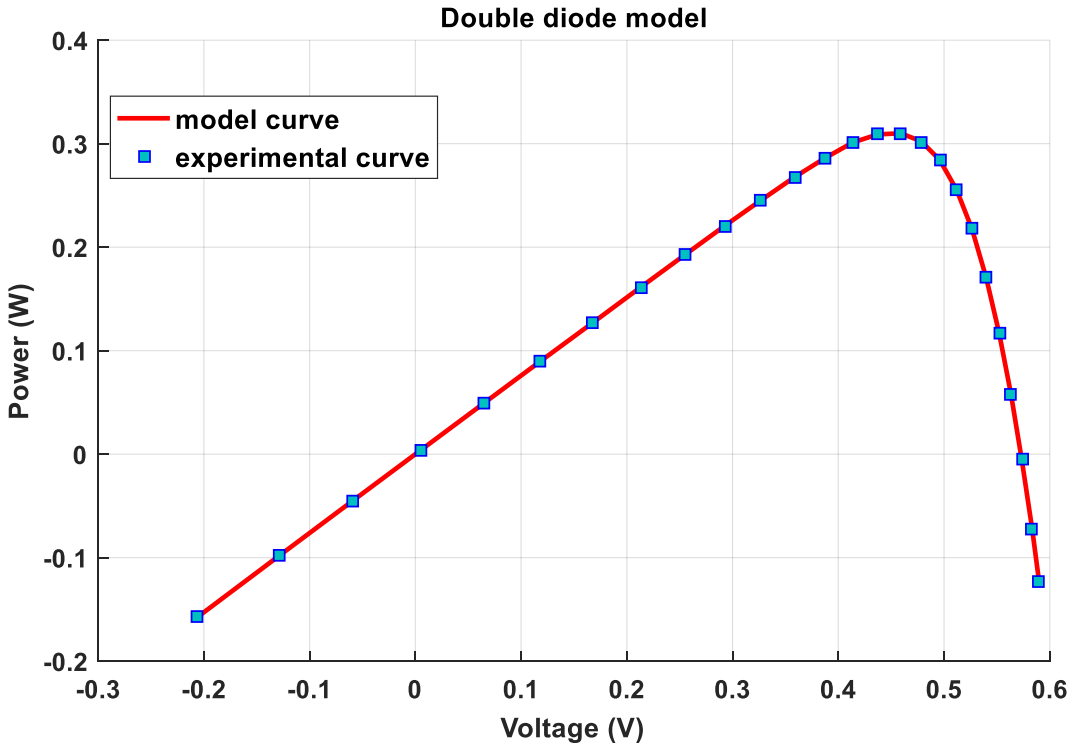

(**b**)

Figure 12. Comparisons between experimental data and simulated data obtained by MGBO for Double diode model (**a**) I-V characteristics; (**b**) P-V characteristics.

4.3. Scenario #3: PV Module Model

For the sake of generality of the MGBO, this subsection will introduce its usage in the PV module model parameters estimation. The estimated parameters of the PV module model using MGBO are given in Table 8. As given in SDM and DDM, the MGBO succeeded to reach the lowest RMSE in a comparatively short time with a comparison with the other comparative algorithms, which can be concluded from Figures 13 and 14, and Table 9. Table 10 lists the IAE of the measured and estimated data points based on the estimated parameters of the PV module model supported by the plot in Figure 15. Besides, the matching between the experimental and simulated quantities is visualized in Figure 16.

Table 8. Best solar cell estimated parameters for the PV module model.

Algorithm	I_{ph} (A)	I_{sd} (μA)	R_s (Ω)	R_{sh} (Ω)	n	RMSE
MGBO	1.030514	3.482263	1.201271	981.9822	48.64283	2.4251×10^{-3}
GBO	1.030514	3.482265	1.201271	981.9827	48.64284	2.4251×10^{-3}
BO	1.030514	3.482263	1.201271	981.9824	48.64283	2.4251×10^{-3}
MRFO	1.03052	3.477694	1.201452	981.0917	48.63778	2.4251×10^{-3}
TLBO	1.030574	3.514497	1.20055	982.9439	48.67867	2.4264×10^{-3}
AEO	1.0305	3.48619	1.201173	984.1829	48.64711	2.4251×10^{-3}

Table 9. Comparisons on the statistical results of different algorithms for PV module model.

Algorithm	RMSE				
	Min	Mean	Median	Max	SD
MGBO	2.4251×10^{-3}	2.4251×10^{-3}	2.4251×10^{-3}	2.4251×10^{-3}	4.73×10^{-9}
GBO	2.4251×10^{-3}	2.4289×10^{-3}	2.4251×10^{-3}	2.4930×10^{-3}	1.52×10^{-5}
BO	2.4251×10^{-3}	2.4897×10^{-3}	2.4251×10^{-3}	2.6189×10^{-3}	9.03×10^{-5}
MRFO	2.4251×10^{-3}	2.4340×10^{-3}	2.4266×10^{-3}	2.4809×10^{-3}	1.58×10^{-5}
TLBO	2.4264×10^{-3}	2.4335×10^{-3}	2.4326×10^{-3}	2.4509×10^{-3}	5.95×10^{-6}
AEO	2.4251×10^{-3}	2.4383×10^{-3}	2.4277×10^{-3}	2.5584×10^{-3}	3.02×10^{-5}

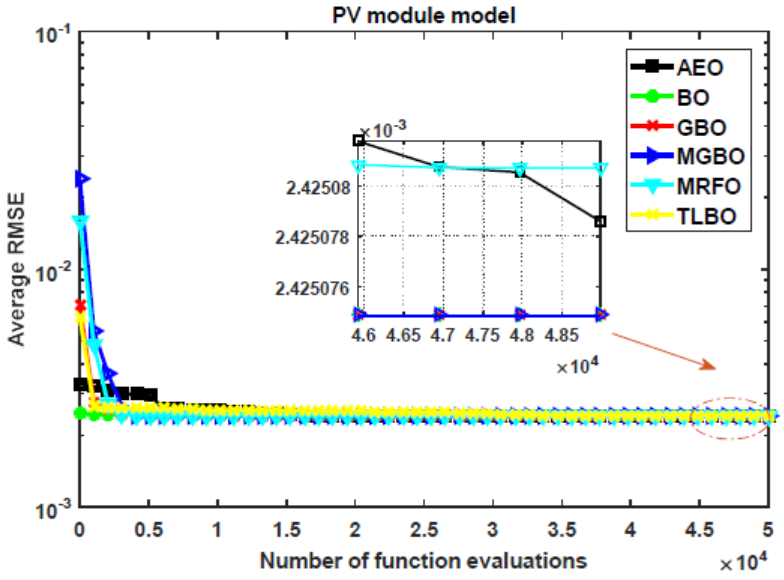

Figure 13. Convergence graphs of different algorithms for the PV module model.

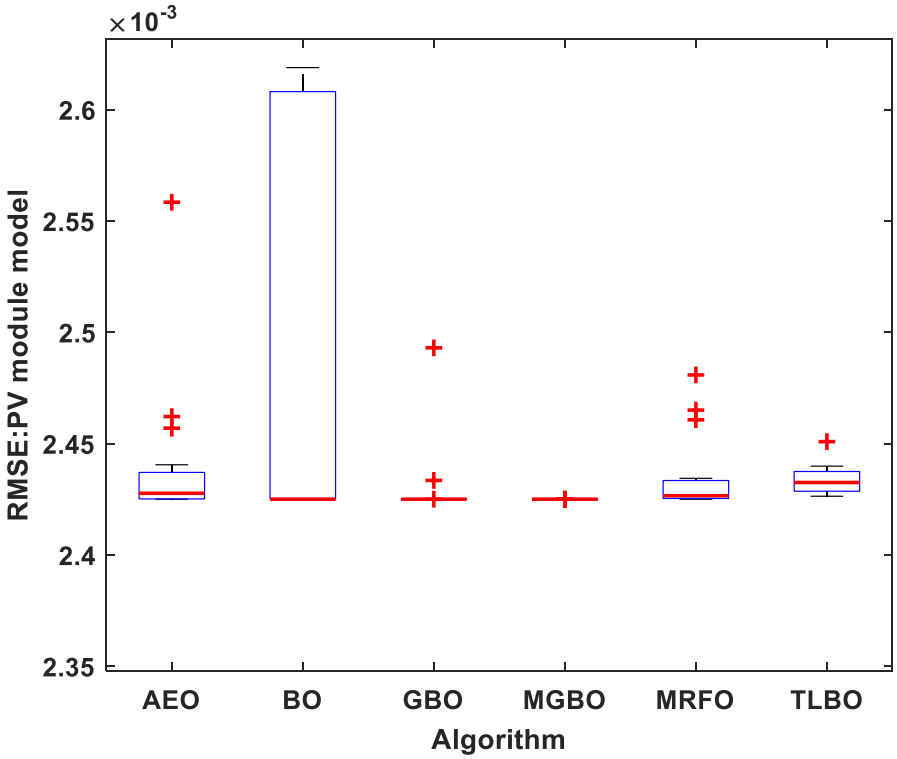

Figure 14. Best RMSE boxplot in 20 runs of different algorithms for the PV module model.

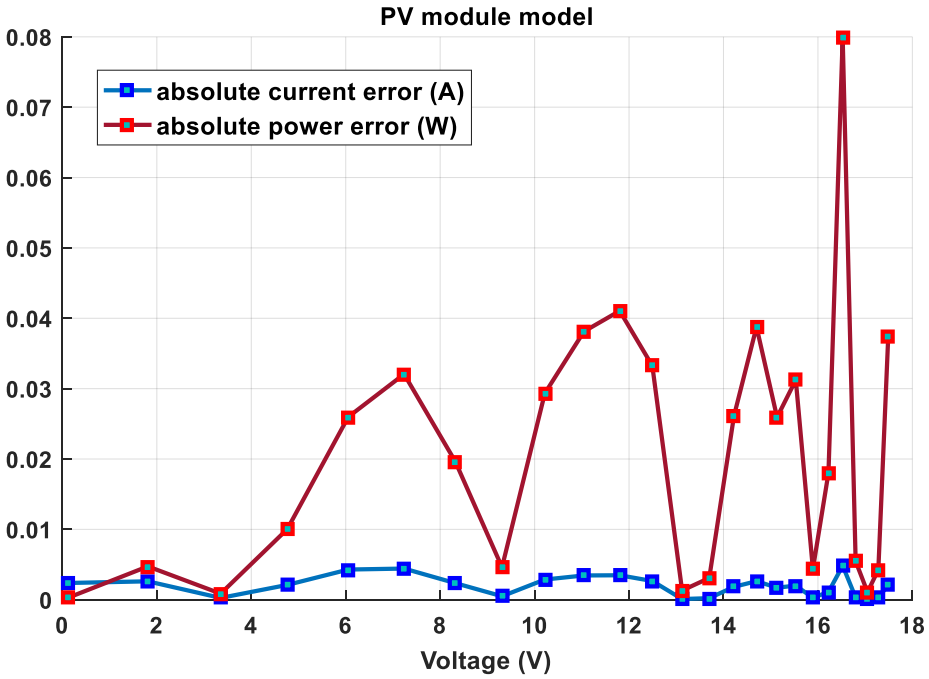

Figure 15. Individual absolute errors for current and power using MGBO (PV module model).

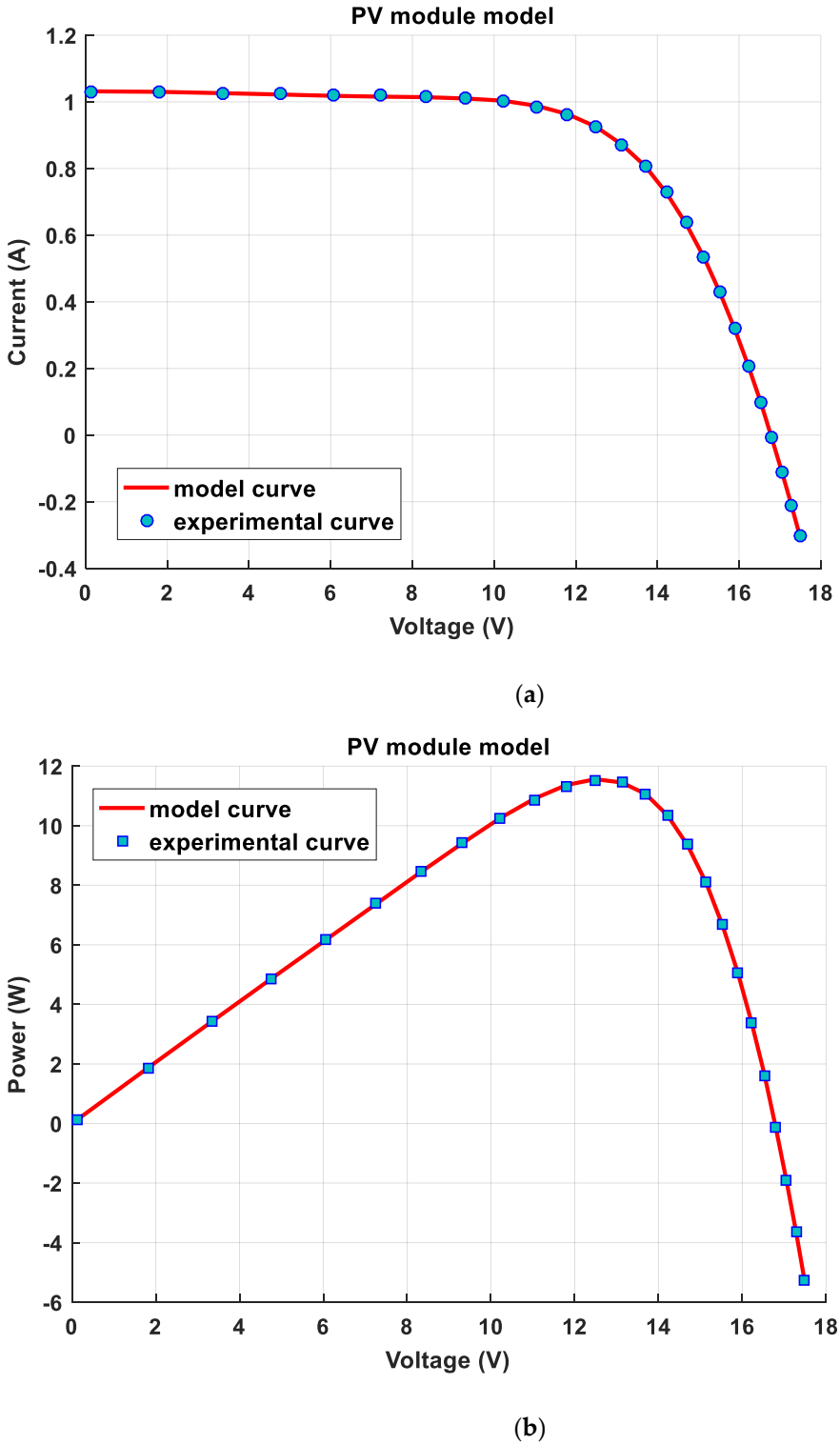

Figure 16. Comparisons between experimental data and simulated data obtained by MGBO for PV module model (**a**) I-V characteristics; (**b**) P-V characteristics.

Table 10. IAE of MGBO on PV module model.

Item	Measured Data			Simulated Current Data		Simulated Power Data	
	V (V)	**I (A)**	**P (w)**	**I_{sim} (A)**	**IAE_I (A)**	**P_{sim} (W)**	**IAE_P (W)**
1	0.1248	1.0315	0.1287312	1.029119162	0.002380838	0.12843407	0.000297129
2	1.8093	1.0300	1.863579	1.027381074	0.002618926	1.85884058	0.004738423
3	3.3511	1.0260	3.4382286	1.025741797	0.000258203	3.43736334	0.000865263
4	4.7622	1.0220	4.8669684	1.024107155	0.002107155	4.87700309	0.010034694
5	6.0538	1.0180	6.1627684	1.022291805	0.004291805	6.18875013	0.025981728
6	7.2364	1.0155	7.3485642	1.019930681	0.004430681	7.38062638	0.032062181
7	8.3189	1.0140	8.4353646	1.016363106	0.002363106	8.45502304	0.019658441
8	9.3097	1.0100	9.402797	1.010496151	0.000496151	9.40741602	0.004619021
9	10.2163	1.0035	10.2520571	1.000628970	0.00287103	10.2227257	0.029331306
10	11.0449	0.9880	10.9123612	0.984548379	0.003451621	10.8742384	0.038122814
11	11.8018	0.9630	11.3651334	0.959521676	0.003478324	11.3240829	0.041050482
12	12.4929	0.9255	11.562179	0.922838818	0.002661182	11.5289331	0.033245880
13	13.1231	0.8725	11.4499048	0.872599663	0.0000996628	11.4512126	0.001307885
14	13.6983	0.8075	11.0613773	0.807274264	0.000225736	11.058285	0.003092204
15	14.2221	0.7265	10.3323557	0.728336478	0.001836478	10.3584742	0.026118573
16	14.6995	0.6345	9.32683275	0.637138000	0.002638	9.36561003	0.038777281
17	15.1346	0.5345	8.0894437	0.536213063	0.001713063	8.11537023	0.025926525
18	15.5311	0.4275	6.63954525	0.429511325	0.002011325	6.67078334	0.031238088
19	15.8929	0.3185	5.06188865	0.318774483	0.000274483	5.06625098	0.004362327
20	16.2229	0.2085	3.38247465	0.207389507	0.001110493	3.36445923	0.018015422
21	16.5241	0.1010	1.6689341	0.096167172	0.004832828	1.58907596	0.079858136
22	16.7987	−0.0080	−0.1343896	−0.00832539	0.000325386	−0.1398557	0.005466062
23	17.0499	−0.1110	−1.8925389	−0.11093648	6.35175E−05	−1.8914559	0.001082966
24	17.2793	−0.2090	−3.6113737	−0.20924727	0.000247266	−3.6156463	0.004272577
25	17.4885	−0.3030	−5.2990155	−0.30086359	0.002136413	−5.2616528	0.037362667
Sum of IAE	-	-	-	-	0.048923675	-	0.516888077

5. Conclusions

In this paper, a novel solution methodology based on a modified version of gradient-based optimizer for extracting the optimal parameters of different photovoltaic models has been presented. A modification to the GBO has been proposed with the aim of enhancing its performance through the integration with the local escaping operator. The MGBO has been used in this research due to its ability to find a global solution, in addition to its fast convergence. A comprehensive comparison has been conducted to prove the superiority of the modified algorithm over the previously used algorithms. Three different equivalent circuit models of PV, single-diode, double-diode, and PV module have been tested with the modified algorithm. The numerical simulation results reflect the capability of the MGBO for parameter extraction of all models with comparatively high precision.

The results obtained by the MGBO have been compared with those obtained by several optimization techniques, GBO, BO, MRFO, TLBO, and AEO. The main finding confirmed the effectiveness of the proposed strategy using MGBO in solving the PV parameter extraction problem compared with the other optimizers. Finally, the enhancement of the MGBO algorithm using chaotic maps will be presented in future work to be used with energy storage systems and fuel cell power generation systems.

Author Contributions: Conceptualization, M.H.H. and S.K.; data curation, M.A.E.-D. and H.R.; formal analysis, M.H.H. and S.K.; resources, M.A.E.-D. and H.R.; methodology, M.H.H. and S.K.; software, M.H.H., S.K., and M.A.E.-D.; supervision, S.K. and H.R.; validation, M.H.H. and M.A.E.-D.; visualization, S.K. and H.R.; writing—original draft, M.H.H. and M.A.E.-D.; writing—review and editing, S.K. and H.R. All authors together organized and refined the manuscript in the present form. All authors have approved the final version of the submitted paper. All authors have read and agreed to the published version of the manuscript.

Funding: This research received no external funding.

Acknowledgments: The authors thank the support of the National Research and Development Agency of Chile (ANID), ANID/Fondap/15110019.

Conflicts of Interest: The authors declare no conflict of interest.

Abbreviations

V_{oc}	Cell/module Open circuit voltage (V)	N	set of measurements
V_m	Cell/module Maximum output voltage (V)	V_t	thermal voltage
I_{sc}	Cell/module short circuit current (A)	I_m	Maximum output current (A)
P_m	Cell/module maximum output power (W)	V	Cell/module output voltage(V)
I_{ph}	photo-generated current (A)	RMSE	Root mean square error
I_{sd}	reverse saturation current (A)	IAE	Integral absolute error
R_{sh}, R_s	Shunt and series resistances.	RE	Relative error
n	ideality factor		
I	Cell/module output current		

References

1. IRENA. *Global Renewables Outlook: Energy transformation 2050*; IRENA: Masdar, United Arab Emirates, 2020.
2. Nunes, H.; Pombo, J.; Bento, P.; Mariano, S.; Calado, M. Collaborative swarm intelligence to estimate PV parameters. *Energy Convers. Manag.* **2019**, *185*, 866–890. [CrossRef]
3. Ayodele, T.; Ogunjuyigbe, A.; Ekoh, E. Evaluation of numerical algorithms used in extracting the parameters of a single-diode photovoltaic model. *Sustain. Energy Technol. Assess.* **2016**, *13*, 51–59. [CrossRef]
4. Qais, M.H.; Hasanien, H.M.; Alghuwainem, S. Identification of electrical parameters for three-diode photovoltaic model using analytical and sunflower optimization algorithm. *Appl. Energy* **2019**, *250*, 109–117. [CrossRef]
5. Ishaque, K.; Salam, Z.; Taheri, H. Accurate MATLAB Simulink PV System Simulator Based on a Two-Diode Model. *J. Power Electron.* **2011**, *11*, 179–187. [CrossRef]
6. Silva, E.A.; Bradaschia, F.; Cavalcanti, M.C.; Nascimento, A.J. Parameter Estimation Method to Improve the Accuracy of Photovoltaic Electrical Model. *IEEE J. Photovolt.* **2015**, *6*, 1–8. [CrossRef]
7. Toledo, F.J.; Blanes, J.M.; Galiano, V. Two-Step Linear Least-Squares Method For Photovoltaic Single-Diode Model Parameters Extraction. *IEEE Trans. Ind. Electron.* **2018**, *65*, 6301–6308. [CrossRef]
8. El Achouby, H.; Zaimi, M.; Ibral, A.; Assaid, E. New analytical approach for modelling effects of temperature and irradiance on physical parameters of photovoltaic solar module. *Energy Convers. Manag.* **2018**, *177*, 258–271. [CrossRef]
9. Elkholy, A.; El-Ela, A.A. Optimal parameters estimation and modelling of photovoltaic modules using analytical method. *Heliyon* **2019**, *5*, e02137. [CrossRef]
10. Louzazni, M.; Khouya, A.; Amechnoue, K.; Mussetta, M.; Crăciunescu, A. Comparison and evaluation of statistical criteria in the solar cell and photovoltaic module parameters' extraction. *Int. J. Ambient. Energy* **2018**, *0750*, 1–13. [CrossRef]
11. Dkhichi, F.; Oukarfi, B.; Fakkar, A.; Belbounaguia, N. Parameter identification of solar cell model using Levenberg–Marquardt algorithm combined with simulated annealing. *Sol. Energy* **2014**, *110*, 781–788. [CrossRef]
12. Bana, S.; Saini, R. Identification of unknown parameters of a single diode photovoltaic model using particle swarm optimization with binary constraints. *Renew. Energy* **2017**, *101*, 1299–1310. [CrossRef]
13. Oliva, D.; Cuevas, E.; Pajares, G. Parameter identification of solar cells using artificial bee colony optimization. *Energy* **2014**, *72*, 93–102. [CrossRef]
14. Zagrouba, M.; Sellami, A.; Bouaïcha, M.; Ksouri, M. Identification of PV solar cells and modules parameters using the genetic algorithms: Application to maximum power extraction. *Sol. Energy* **2010**, *84*, 860–866. [CrossRef]
15. Ma, J.; Ting, T.O.; Man, K.L.; Zhang, N.; Guan, S.-U.; Wong, P.W.H. Parameter Estimation of Photovoltaic Models via Cuckoo Search. *J. Appl. Math.* **2013**, *2013*, 1–8. [CrossRef]
16. Chen, X.; Yu, K. Hybridizing cuckoo search algorithm with biogeography-based optimization for estimating photovoltaic model parameters. *Sol. Energy* **2019**, *180*, 192–206. [CrossRef]
17. Augusto, R.; Franco, P.; Filho, G.L.; Henrique, F.; Vieira, T. *Firefly Algorithm Applied to the Estimation of the Parameters of a Photovoltaic Panel Model*; Springer International Publishing: Cham, Switzerlan, 2019.
18. Allam, D.; Yousri, D.; Eteiba, M. Parameters extraction of the three diode model for the multi-crystalline solar cell/module using Moth-Flame Optimization Algorithm. *Energy Convers. Manag.* **2016**, *123*, 535–548. [CrossRef]
19. Ram, J.P.; Babu, T.S.; Dragicevic, T.; Rajasekar, N. A new hybrid bee pollinator flower pollination algorithm for solar PV parameter estimation. *Energy Convers. Manag.* **2017**, *135*, 463–476. [CrossRef]
20. Beigi, A.M.; Maroosi, A. Parameter identification for solar cells and module using a Hybrid Firefly and Pattern Search Algorithms. *Sol. Energy* **2018**, *171*, 435–446. [CrossRef]
21. Askarzadeh, A.; Rezazadeh, A. Parameter identification for solar cell models using harmony search-based algorithms. *Sol. Energy* **2012**, *86*, 3241–3249. [CrossRef]

22. Han, W.; Wang, H.-H.; Chen, L. Parameters Identification for Photovoltaic Module Based on an Improved Artificial Fish Swarm Algorithm. *Sci. World J.* **2014**, *2014*, 1–12. [CrossRef]
23. Kanimozhi, G.; Kumar, H. Modeling of solar cell under different conditions by Ant Lion Optimizer with LambertW function. *Appl. Soft Comput.* **2018**, *71*, 141–151. [CrossRef]
24. Kler, D.; Sharma, P.; Banerjee, A.; Rana, K.; Kumar, V. PV cell and module efficient parameters estimation using Evaporation Rate based Water Cycle Algorithm. *Swarm Evol. Comput.* **2017**, *35*, 93–110. [CrossRef]
25. Yu, K.; Qu, B.; Yue, C.; Ge, S.; Chen, X.; Liang, J. A performance-guided JAYA algorithm for parameters identification of photovoltaic cell and module. *Appl. Energy* **2019**, *237*, 241–257. [CrossRef]
26. Kler, D.; Goswami, Y.; Rana, K.; Kumar, V. A novel approach to parameter estimation of photovoltaic systems using hybridized optimizer. *Energy Convers. Manag.* **2019**, *187*, 486–511. [CrossRef]
27. Jacob, B.; Balasubramanian, K.; Thanikanti, S.B.; Azharuddin, S.M.; Rajasekar, N. Solar PV Modelling and Parameter Extraction Using Artificial Immune System. *Energy Procedia* **2015**, *75*, 331–336. [CrossRef]
28. Abbassi, R.; Abbassi, A.; Heidari, A.A.; Mirjalili, S. An efficient salp swarm-inspired algorithm for parameters identification of photovoltaic cell models. *Energy Convers. Manag.* **2019**, *179*, 362–372. [CrossRef]
29. Niu, Q.; Zhang, L.; Li, K. A biogeography-based optimization algorithm with mutation strategies for model parameter estimation of solar and fuel cells. *Energy Convers. Manag.* **2014**, *86*, 1173–1185. [CrossRef]
30. Zaky, A.A.; El Sehiemy, R.A.; Rashwan, Y.I.; Elhossieni, M.A.; Gkini, K.; Kladas, A.; Falaras, P. Optimal Performance Emulation of PSCs using the Elephant Herd Algorithm Associated with Experimental Validation. *ECS J. Solid State Sci. Technol.* **2019**, *8*, Q249–Q255. [CrossRef]
31. Hachana, O.; Hemsas, K.E.; Tina, G.M.; Ventura, C. Comparison of different metaheuristic algorithms for parameter identification of photovoltaic cell/module. *J. Renew. Sustain. Energy* **2013**, *5*, 053122. [CrossRef]
32. Chen, Z.; Wu, L.; Lin, P.; Wu, Y.; Cheng, S. Parameters identification of photovoltaic models using hybrid adaptive Nelder-Mead simplex algorithm based on eagle strategy. *Appl. Energy* **2016**, *182*, 47–57. [CrossRef]
33. Jiang, L.L.; Maskell, D.L.; Patra, J.C. Parameter estimation of solar cells and modules using an improved adaptive differential evolution algorithm. *Appl. Energy* **2013**, *112*, 185–193. [CrossRef]
34. Yuan, X.; He, Y.; Liu, L. Parameter extraction of solar cell models using chaotic asexual reproduction optimization. *Neural Comput. Appl.* **2014**, *26*, 1227–1239. [CrossRef]
35. Gao, X.; Cui, Y.; Hu, J.; Xu, G.; Wang, Z.; Qu, J.; Wang, H. Parameter extraction of solar cell models using improved shuffled complex evolution algorithm. *Energy Convers. Manag.* **2018**, *157*, 460–479. [CrossRef]
36. Yousri, D.; Allam, D.; Eteiba, M.; Suganthan, P.N. Static and dynamic photovoltaic models' parameters identification using Chaotic Heterogeneous Comprehensive Learning Particle Swarm Optimizer variants. *Energy Convers. Manag.* **2019**, *182*, 546–563. [CrossRef]
37. Yuan, X.; Xiang, Y.; He, Y. Parameter extraction of solar cell models using mutative-scale parallel chaos optimization algorithm. *Sol. Energy* **2014**, *108*, 238–251. [CrossRef]
38. Zhao, W.; Wang, L.; Zhang, Z. Artificial ecosystem-based optimization: A novel nature-inspired meta-heuristic algo-rithm. *Neural. Comput. Appl.* **2020**, *32*, 9383–9425. [CrossRef]
39. Soliman, M.A.; Hasanien, H.M.; Alkuhayli, A. Marine Predators Algorithm for Parameters Identification of Triple-Diode Photovoltaic Models. *IEEE Access* **2020**, *8*, 155832–155842. [CrossRef]
40. Ramadan, A.; Kamel, S.; Korashy, A.; Yu, J. Photovoltaic Cells Parameter Estimation Using an Enhanced Teaching–Learning-Based Optimization Algorithm. *Iran. J. Sci. Technol. Trans. Electr. Eng.* **2019**, *44*, 767–779. [CrossRef]
41. Qais, M.H.; Hasanien, H.M.; Alghuwainem, S.; Nouh, A.S. Coyote optimization algorithm for parameters extraction of three-diode photovoltaic models of photovoltaic modules. *Energy* **2019**, *187*, 116001. [CrossRef]
42. Qais, M.H.; Hasanien, H.M.; Alghuwainem, S. Parameters extraction of three-diode photovoltaic model using computation and Harris Hawks optimization. *Energy* **2020**, *195*, 117040. [CrossRef]
43. ElAzab, O.S.; Hasanien, H.M.; Alsaidan, I.; Abdelaziz, A.Y.; Muyeen, S.M. Parameter Estimation of Three Diode Photovoltaic Model Using Grasshopper Optimization Algorithm. *Energies* **2020**, *13*, 497. [CrossRef]
44. Jordehi, A.R. Gravitational search algorithm with linearly decreasing gravitational constant for parameter estimation of photovoltaic cells. In Proceedings of the 2017 IEEE Congress on Evolutionary Computation (CEC), San Sebastian, Spain, 5–8 June 2017; pp. 37–42. [CrossRef]
45. Sheng, H.; Li, C.; Wang, H.; Yan, Z.; Xiong, Y.; Cao, Z.; Kuang, Q. Parameters Extraction of Photovoltaic Models Using an Improved Moth-Flame Optimization. *Energies* **2019**, *12*, 3527. [CrossRef]
46. Lockett, A.J. No Free Lunch Theorems. *Lect. Notes Comput. Sci.* **2020**, *1*, 287–322. [CrossRef]
47. Diab, A.A.Z.; Sultan, H.M.; Aljendy, R.; Al-Sumaiti, A.S.; Shoyama, M.; Ali, Z.M. Tree Growth Based Optimization Algorithm for Parameter Extraction of Different Models of Photovoltaic Cells and Modules. *IEEE Access* **2020**, *8*, 119668–119687. [CrossRef]
48. Merenda, M.; Iero, D.; Carotenuto, R.; Della Corte, F.G. Simple and Low-Cost Photovoltaic Module Emulator. *Electronics* **2019**, *8*, 1445. [CrossRef]
49. Zafar, M.H.; Al-Shahrani, T.; Khan, N.M.; Mirza, A.F.; Mansoor, M.; Qadir, M.U.; Khan, M.I.; Naqvi, R.A. Group Teaching Optimization Algorithm Based MPPT Control of PV Systems under Partial Shading and Complex Partial Shading. *Electronics* **2020**, *9*, 1962. [CrossRef]

50. Chin, V.J.; Salam, Z. A New Three-point-based Approach for the Parameter Extraction of Photovoltaic Cells. *Appl. Energy* **2019**, *237*, 519–533. [CrossRef]
51. Ahmadianfar, I.; Bozorg-Haddad, O.; Chu, X. Gradient-based optimizer: A new metaheuristic optimization algorithm. *Inf. Sci.* **2020**, *540*, 131–159. [CrossRef]
52. Oliva, D.; Rodriguez-Esparza, E.; Martins, M.S.R.; Elaziz, M.A.; Hinojosa, S.; Ewees, A.A.; Lu, S. Balancing the Influence of Evolutionary Operators for Global optimization. In Proceedings of the 2020 IEEE Congress on Evolutionary Computation (CEC), Glasgow, UK, 19–24 July 2020; pp. 1–8.
53. Korashy, A.; Kamel, S.; Youssef, A.-R.; Jurado, F. Modified water cycle algorithm for optimal direction overcurrent relays coordination. *Appl. Soft Comput.* **2019**, *74*, 10–25. [CrossRef]